REVISTA MATÉRIA V.27 N.01

ISSN 1517-7076 articles e13158, 2022

Application of lithium nonafluoro-1-butane sulfonate (nonaflate) based non-aqueous liquid electrolytes (NALE) in lithium-ion batteries

Hirankumar Gurusamy[1],
Sakunthala Ayyasamy[2], Daries Bella[3]

[1]Department of Physics, Ramakrishna Mission Vivekananda College, Chennai 600 004, Tamil Nadu, India
[2]Solid State Ionics Lab, Department of Applied Physics, Karunya Institute of Technology and Sciences, Coimbatore 641 114, Tamil Nadu, India
[3]Department of Physics, Stella Maris College, Chennai 600 086, Tamil Nadu, India
Email: g.hirankumar@rkmvc.ac.in

ABSTRACT

The non-aqueous electrolyte system comprising of the lithium nonafluoro-1-butane sulfonate (LiNfO) as a potential lithium ion-conducting salt in an equivalent binary mixture of propylene carbonate (PC) and 1, 2-dimethoxyethane (DME) as the solvent was explored for the lithium battery applications. The LiNfO based non-aqueous liquid electrolyte (NALE) system showed the highest ionic conductivity of 2.66 x 10^{-3} S cm^{-1} at ambient temperature, and a potential window stability of ~5 V. The lithium ion cells, Li/NALE//$LiCoO_2$ were fabricated with the proposed non-aqueous electrolyte. The cell with particular composition of electrolyte delivered a high specific discharge capacity of 154 mA h g^{-1} at ambient temperature. The potential advantages of the proposed NALE are discussed in detail.

Keywords: electrolyte, lithium ionic conductivity, electrochemical properties, impedance spectroscopy

1. INTRODUCTION

Though new battery systems are evolving, the research on Lithium ion Batteries (LIBs) is an evergreen area of research interest due to its specific property of high voltage and high energy density [1-3], which cannot be matched with other battery systems for portable electronic applications. So far, in LIBs, the electrolytes containing the $LiPF_6$ salt in EC/PC/DMC are mostly used due to its high conductivity and better electrochemical stability [4]. However, when the above electrolyte is used, the formation of HF during de-intercalation/intercalation leads to the poor performance of the cells [5] and hence for long storage times, it is unsuitable. Moreover, it also shows the thermal instability. Hence, considerable efforts have been made to replace $LiPF_6$ with other conventional lithium salts. ZHANG *et al.* [6], prepared a new family of Fluorosulfonimide anions, i.e., bis(fluorosulfonyl)imide, $[(FSO_2)_2N]^-$, and (fluorosulfonyl)(perfluoroalkanesulfonyl)imide, $[(FSO_2)(n\text{-}C_mF_{2m+1}SO_2)N]^-$ (m = 1, 2, 4, 6, 8), and their alkali metal salts. Lithium salts with fluorosulfonimide anions show good thermal, chemical, and electrochemical stability, and do not contain HF. However, the heavy corrosion behavior at the aluminium current collector on the cathode side (around 3.3 V vs Li/Li^+) restricts its application range.

Fortunately, one of the newest fluoro-lithium salt, lithium nonafluoro-1-butane sulfonate ($LiSO_3C_4F_9$) has a weak cation-anion interaction and appreciably larger anion size compared to other leading lithium salts such as $LiClO_4$, $LiSO_3CF_3$, and $LiPF_6$ [7, 8]. The anionic size of the lithium salt has influenced the dissolution property, which in turn facilitate the number of charge carriers, diffusion coefficient and conductivity of the electrolytes [9]. Also, the proposed new lithium salt LiNfO possesses much greater thermal and electrochemical stabilities and will be the perfect alternate for $LiPF_6$ in commercial batteries.

But, in such non-aqueous liquid electrolytes (NALEs) system, the selection of the solvent for incorporating the salt plays a vital role on the electrochemical properties of LIBs. The high dielectric constant and low viscosity of solvents are generally desirable. Among the different carbonate based solvents, propylene carbonate (PC) exhibits excellent properties such as high dielectric constant (64.92) and wide

Corresponding Author: Hirankumar Gurusamy Received on: 25/05/2021 Accepted on: 25/10/2021

10.1590/S1517-707620220001.1358

electrochemical stability window [10, 11]. Therefore, the blending of propylene carbonate with 1,2-dimethoxy ethane (DME) with the dielectric constant and the viscosity values of 7.2 and 0.46 *cP* respectively, may synergistically enhance the conductivity and electrochemical stability of LIBs [12]. Hence in the present investigation, we have chosen PC and DME as binary solvent mixture for LIBs. Few of the reports below show the trends in electrolyte research for Li/$LiCoO_2$ cells. KONG *et al.* [13], have reported that, the electrolyte with 1M $LiPF_6$ in dimethyl sulfone (DMS) as a solvent increases the capacity retention rate from the original 38.1% up to 87.1% after cycling for 300 times at 4.45 V for the Li/$LiCoO_2$ cell. Mostly Li/$LiCoO_2$ cells are cycled up to a high operating voltage of 4.0 V vs Li [14], and the above report shows that the voltage window of Li/$LiCoO_2$ cell could be enhanced by the selection of suitable electrolyte. HONG-BO HAN *et al.* [15], prepared the electrolyte of 1.0 M Lithium bis(fluorosulfonyl)imide LiFSI–EC/EMC (3:7, v/v) and compared the Li/$LiCoO_2$ cell performance with typical lithium salt of $LiPF_6$ in similar solvent concentration and reported the role of electrolyte. The main objective of the present work is to prepare a new category of NALEs systems for LIBs by varying the volume ratio of the binary solvents and lithium salt LiNfO. We observed that the prepared NALEs show better conductivity, electrochemical stability and cationic transference number. In addition, NALEs using LiNfO presented a promising performance in terms of cycle life and rate capability when tested in LIBs using Li//$LiCoO_2$ electrode.

2. MATERIALS AND METHODS

2.1 Materials

The precursor solvents such as anhydrous propylene carbonate (PC, 99.7 %), anhydrous dimethoxyethane (DME, 99.5 %) were purchased from Sigma Aldrich and were used without any further purification. The lithium salt LiNfO (95 %) was obtained from the TCI Chemicals. The lithium cobalt oxide material was obtained from Sigma Aldrich and used as such. A series of non-aqueous liquid electrolytes were prepared by dissolving 0.1 M LiNfO in the PC/DME binary solvent mixture (Table 1) and used for determining the Li//$LiCoO_2$ cell performance.

2.2 Coin cell Assembly

The cathode slurry was prepared by mixing the stoichiometric ratio of $LiCoO_2$, acetylene black and poly(vinylidene fluoride) (PVdF), in the ratio of 80:10:10 in N-methyl-2-pyrrolidone (NMP) until smooth slurry was formed. The slurry was then coated on an aluminum foil using doctor blade coating machine. The coated aluminum sheet was dried in vacuum oven for 12 h at 120 °C and then pressed by a rolling machine and taken as the electrode. Lithium was used as both the reference and counter electrode in the half-cells. A monolayer polypropylene membrane (Celgard # PP2075, thickness of 20 µm, porosity of 48 %) was used as a potential cell separator. Both the preparation of NALEs and the fabrication of half-cells (both Swagelok and coin) were carried out in an argon filled glove box, where the moisture and oxygen level were maintained less than 1 ppm.

2.3 Electrical and Electrochemical studies

The conductivity of NALEs were measured using conductivity meter (Systronics, Model: conductivity meter-306) (cell constant K=1.0±10 %) with platinum electrodes. The linear sweep voltammetry (LSV) of the cell was done at a scan rate of 5 mV s^{-1}. The high conducting NALE was used to examine the cationic transference number using combination measurement of AC impedance and DC polarization techniques. For this measurement, the symmetric Swagelok cells (Li|high conducting NALE electrolyte|Li) were assembled using lithium electrodes. The impedance spectra were measured using dc polarization technique in the frequency range between 100 mHz and 100 kHz with a signal amplitude of 10 mV. For DC polarization measurement, the constant dc voltage of 20 mV was applied for 8 hours to reach the steady state current. The above characterization techniques of LSV, DC polarization technique, CV, Charge-Discharge and Electrochemical Impedance Spectroscopy (EIS) were carried out by using electrochemical workstation of Bio-Logic sp-300 (France).

3. RESULTS AND DISCUSSION

3.1 Electrical properties

The ionic conductivity of LiNfO/PC/DME NALEs were evaluated by AC ionic conductivity measurement. The ionic conductivity of 0.1 M solution of LiNfO in different volumetric ratio (by v %) of PC and DME binary solvents are shown in Figure 1 (a). As well as, its corresponding conductivity values and volumetric ratios of binary solvents are tabulated in the Table 1. As it can be seen from the Figure 1 (a) and the Table 1, the ionic conductivity of all the prepared NALEs is in the range of mS cm^{-1}. Amongst all the prepared NALEs, NALE 5 and NALE 1 shows the highest ionic conductivity at ambient temperature which is owing to the solvating ability of DME over PC (DME>PC) which in turn means the greater difference in donor number between DME (26.6) and PC (15.1) [16]. The obtained results for 0.1 M NALE solution are higher compared to other liquid electrolytes and strongly concurrent with the earlier reported results [17-19].

In order to validate the conductivity results as well as to confirm the migration of the ions in NALEs system, we have performed the chronoamperometry analysis for the high conducting sample NALE 1. The Nyquist impedance plot for NALE 1 before and after polarization is shown in Figure 1 (b) and the arrow indicates the direction of the increase in the frequency. It consists of two compressed semicircles at high and medium frequencies and an inclined peak at low frequency. The first semicircle touches Z' at medium frequency with highest resistivity while the second semicircle touches at higher frequency and lower resistivity. The compressed semicircle at high and medium frequencies may attribute to the grain boundary impedance in charge of the transfer process whereas the inclined peak at low frequency is related to the diffusion process. The resistances R_o and R_s were evaluated from the intercept of the semicircle with real axis (Z') of the Nyquist plot. The cationic transference number was calculated by means of following expression [20] and mentioned in Table 2.

$$T_{Li^+} = \frac{I_s\,(\Delta V - I_0 R_0)}{I_0\,(\Delta V - I_s R_s)} \tag{1}$$

Where ‘I_0’ and ‘I_s’ are initial and final steady state current, respectively (Figure 1 (c)). Here, ‘ΔV’ is the applied constant potential (20 mV). Further, it seems from the impedance plot that the resistance became higher after the polarization when compared to fresh cell which was due to the formation of an interfacial layer between the lithium electrode and electrolyte. Its corresponding equivalent circuit is shown as insert Figure 1 (b). The cationic transference number was determined using the above formula and it was found to be 0.39. The observed transference number value clearly demonstrates that the charge transport in NALE 1 is mainly due to the movable lithium ions and hence this electrolyte is a pretty potential candidate as electrolyte in LIBs. The obtained results are in concurrent with the earlier reported result by ZUGMANN *et al.* [21] for $LiPF_6$ in EC/DEC.

Table 1: Conductivity and Electrolyte stability potential for 0.1M of NALEs

NALE	RATIO OF PC: DME	CONDUCTIVITY mS cm^{-1}	DECOMPOSITION POTENTIAL at 0.1 mA (VOLT)
NALE 1	1v%:1v%	2.65	5
NALE 2	1v%:2v%	2.55	4.6
NALE 3	1v%:3v%	2.26	4.5
NALE 4	2v%:1v%	2.40	4.9
NALE 5	2v%:3v%	2.66	4.7
NALE 6	3v%:1v%	2.18	5
NALE 7	3v%:2v%	2.54	5.3

Table 2: Cationic transference number from chronoamperometry studies for the NALE 1 electrolyte system

SAMPLE	I_o	I_s	R_o	R_s	$T_{Li^+} = \frac{I_s}{I_o}$	$T_{Li^+} = \frac{I_s(\Delta V - I_o R_o)}{I_o(\Delta V - I_s R_s)}$
NALE 1	0.45	0.18	2.72	2.96	0.4	0.39

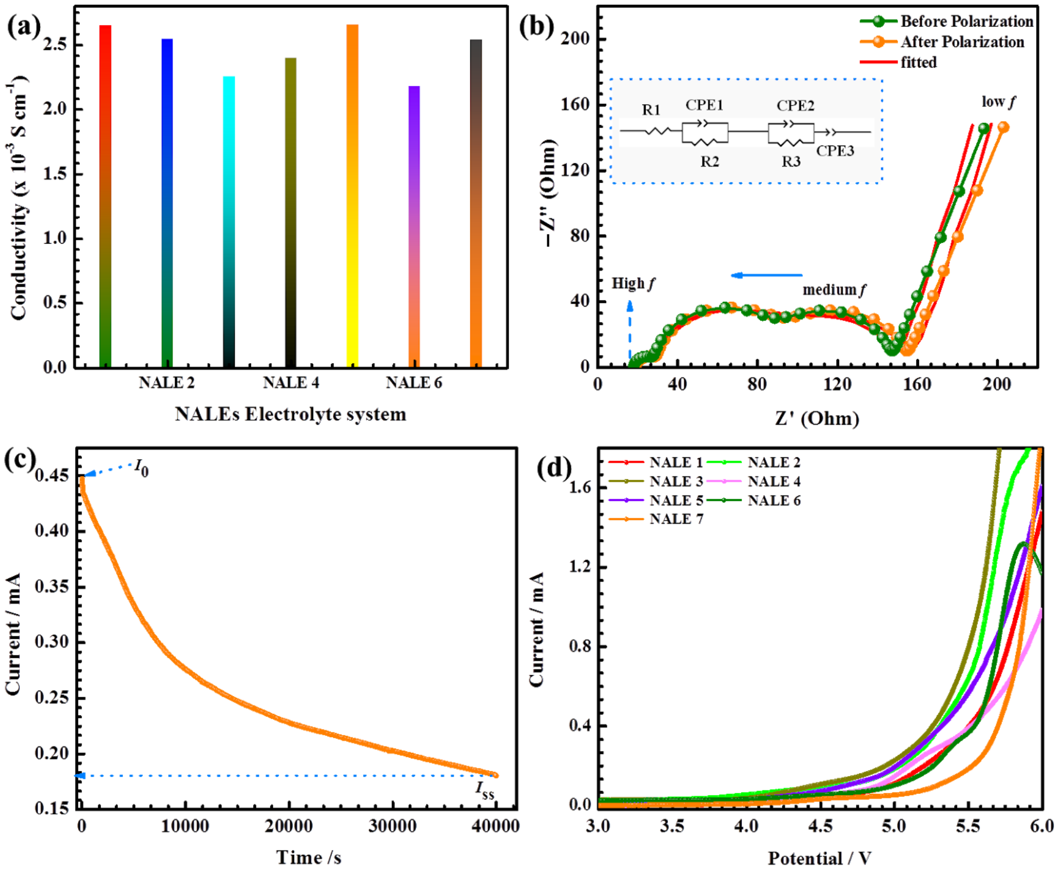

Figure 1: (a) Conductivity plot of different NALEs system, (b) Impedance spectra before and after polarization measurement, (c) Chronoamperometry studies for the NALE 1 system and the (d) LSV curves of SS/NALE 1/Li cell

3.2 Electrochemical Stability

In order to find the electrochemical stability window of the prepared NALEs system, the coin cell (SS/NALEs/Li) was subjected to linear sweep voltammetry analysis. In general, the electrochemical stability window of liquid electrolyte system depends on the nature of the salt, solvent and electrode materials [22-24]. In order to determine the effect of solvent/solvent mixture in the NALEs system, the analysis was performed with similar types of electrodes. Hence, electrochemical stability window is expected to depend only on the nature of the salt and solvent. In the present investigation, we have optimized and fixed the cut-off current as 0.1 mA. Figure 1 (d) shows the linear sweep voltammogram of different NALEs which consists of various volumetric ratios of PC and DME. As it can be seen from the Figure 1 (d) that the I-V curve displays almost no residual current in the anodic decomposition voltage, postulating the high purity of the NALEs which is electrochemically sensitive to impurities. Henceforth, the anodic current detected in the curve elucidates the oxidation of NfO− which is the anion of the employed lithium salt [8]. The obtained decomposition potential of all the NALEs is given in the Table 1. Amongst, NALE 7 was electrochemically stable for a long time and shows the decomposition potential at 5.3 V. Whereas, in the case of NALE 2, NALE 3 and NALE 5 electrolytes the decomposition potential were 4.6, 4.5 and 4.7 V respectively. This is due to the fact that the solvent DME which is an ether compound and decomposed even at a lower potential than PC [25, 26]. The high conducting NALE 1 electrolyte showed a maximum stability voltage of 5 V, making it suitable for battery applications. The obtained results strongly suggest a way to utilize the NALEs system as potential candidates for the application in all state-of-the-art electrode materials for LIBs.

3.3 Cyclic Voltammetry analysis

In order to validate the reversible nature of prepared NALE system, the $LiCoO_2$/NALE 1/Li coin cell was subjected to cyclic voltammetry analysis. The resulting cyclic voltammogram is shown in the Figure 2.

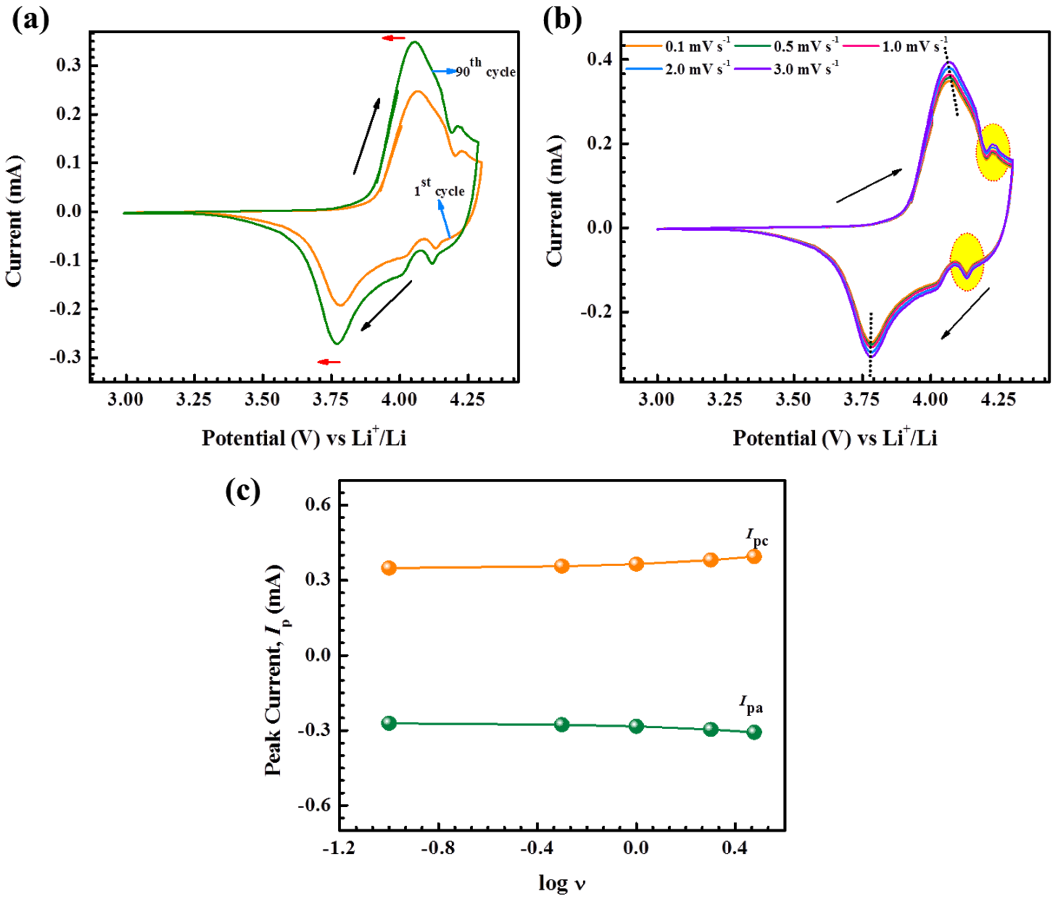

Figure 2: (a) CV curve of Li//NALE 1// $LiCoO_2$ before and after cycling (Scan rate: 0.1 mV/s), (b) CV curve of Li//NALE 1// $LiCoO_2$ at different scan rates (c) Peak current (I_p) as a function of logarithmic scan rate for Li//NALE 1// $LiCoO_2$

The reason for choosing NALE 1 electrolyte is owing to its high ionic conductivity and potential stability as discussed so far. Figure 2 (a) represents the CV curve of fresh coin cell (i.e. before cycling) in the potential range between 3 and 4.3 V at room temperature at a scan rate 0.1 mV s^{-1}. In the case of fresh cell, the first-cycle anodic scan, the main peak occurs at 4.05 V (versus Li) due to de-intercalation of Li ions and the corresponding peak in cathodic scan was at 3.77 V due to intercalation of Li ions. It is widely recognized that the difference between the anodic and cathodic peak voltages (ΔV) relates to the degree of polarization [27]. The ΔV value of 0.29 V was obtained for a fresh cell indicating good reversibility of the charge-discharge reaction. Favorably, the CV showed that, even after 90 cycles, the ΔV remains almost constant. Two more small peaks at 4.17 and 4.21 V were appeared in the CV of fresh cell during the anodic scan. The corresponding cathodic peaks were at 4.01, and 4.13 V. These can be assigned to the reversible phase transitions of Hexagonal (H) ↔ Monoclinic (M) in $LiCoO_2$. Similar behavior of CV of $LiCoO_2$ was reported in literatures [28, 29]. Whereas, the prolonged (after 90 cycles) cycled cell also shows a similar type of redox peak with slight changes in which the peaks are shifted towards left. The structural degradations of $LiCoO_2$ in the entire cycling lead to capacity fading in the cell [30, 31]. In addition, it is interesting to note that the cycled cell has higher peak current than that of the fresh cell. However, the presence of clear oxidation and reduction peaks have proved the good reversibility of lithium ion over the fixed potential range [32, 33]. The reversibility of the cell will be further strengthened by Laviron's theory [3, 34] as discussed below,

The CV response towards the electrochemical redox reaction of Li//NALE 1// $LiCoO_2$ at different scan rates between 0.1 and 3 mV s^{-1} is displayed in Figure 2 (b). It seems that there is no alteration in the CV's even at high scan rates indicating the fast intercalation –de intercalation behavior. Also, the value of anodic and cathodic currents increases with increase in scan rate and it doesn't follow a linear shape as shown in Figure 2 (c). According to Laviron's theory, the linear shape curves are obtained only at high scan rates (>20 mV s^{-1}) [7]. The ratio of anodic peak current to the cathodic peak current is nearly 1 and the positions of anodic and cathodic currents not shifted much as considerable potentials at different scan rates which are confirmed the good reversible reaction of the cell [35]. Hence to conclude that the cathodic deposition and anodic oxidation are facetious at the electrolyte-electrode interfaces and so are investigative of lithium ion conduction in the NALE 1. The obtained results are further strengthened by charge discharge analysis which will be discussed later in the following sections.

3.4 Galvanostatic charge-discharge analysis

It is well recognized that the galvanostatic charge discharge measurement is the most trustworthy and precise method for evaluating the specific capacity of LIB's components compared to both CV and impedance methods [36, 37]. Figure 3 (a) shows the discharge characteristic profiles obtained for $LiCoO_2$/NALE 1/Li coin cell at different C-rates such as 0.1, 0.2, 0.5 and 1 C. Since the rate capability is an important factor for battery performance, the coin cell comprising of NALE 1 electrolyte was subjected to a preconditioning cycle with a cut off voltage of charge and discharge between 3.0 and 4.3 V before the execution of the rate capability test at 0.1 C rates. As it can be observed from the Figure 3 (a) that the cycling performance at 0.1 C-rate with a discharge capacity of 154 mA h g^{-1} is concededly good. Further, the discharge capacity at 0.2, 0.5 and 1 C rates were 143.12, 119.22 and 44.9 mA h g^{-1}, respectively for their first initial cycles. This was about 96 - 28% of the theoretical capacity of the active electrode $LiCoO_2$ (160 mA h g^{-1}) [38, 39]. The obtained results show that the discharge capacity and the efficiency decreased with increasing C- rate [40, 41] and the capacity fading at higher current rates occur faster than at lower discharge rates as shown in Figure 3 (b). Additionally, the discharge profile clearly shows voltage plateau at ~ 4.1 V which corresponding to the phase transition of Hexagonal (H) ↔ Monoclinic (M) in $LiCoO_2$. They were observed as a minor peaks in the CV curves at 4.01 V and 4.13 V and these results are quite similar as reported by Szu Lui Tey [29].

Further, the stability of the prepared NALE 1 electrolyte is equitably good. For instance, the cell run at 0.2 C rate between the voltage range of 3 and 4.3 V provides an initial discharge capacity of 143 mA h g^{-1} and still maintained 31.41 mAh g^{-1} capacity after 90 cycles as shown in Figure 3 (c). Its corresponding coulombic efficiency curve as displayed in Figure 3 (d) was 68 % during 1st cycle and attained 98 % after 90th cycle which clearly represents the better capacity retention nature of the cell. The capacity fade was mainly associated with the phase transitions of $LiCoO_2$ above 4.1 V [42, 43] which has evident through the CV result. The results are consistent with the earlier work [39]. Moreover, the coulombic efficiency values slowly increased and stabilized after few cycles. This may be due to the formation of electrode and electrolyte interfaces [27].

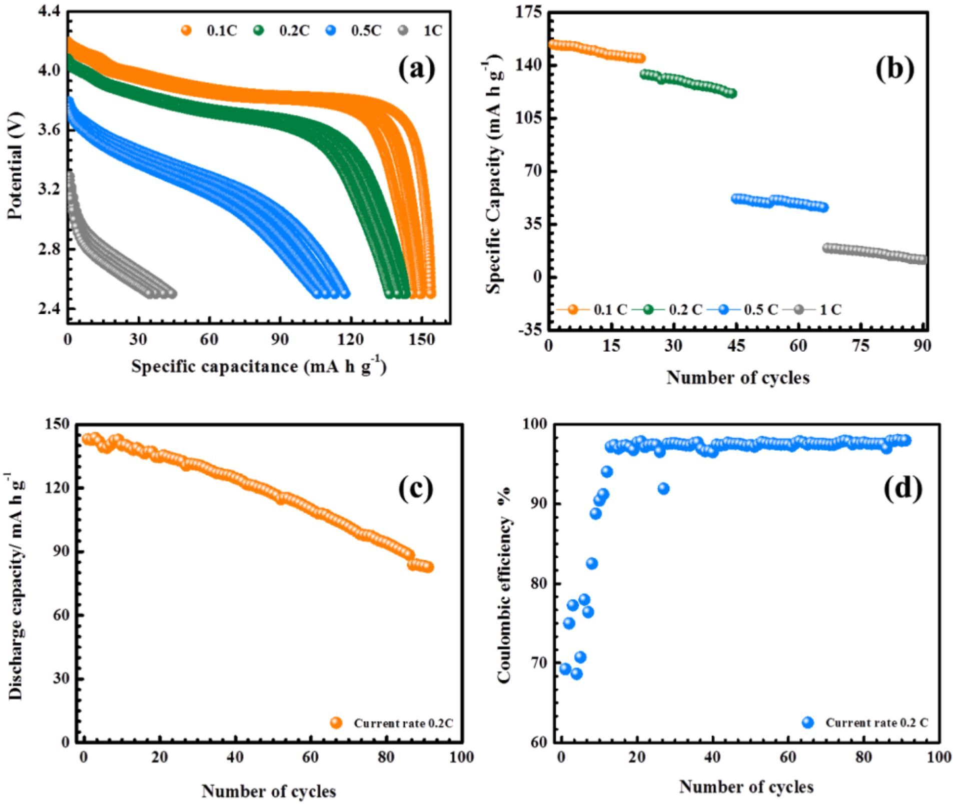

Figure 3: (a) Discharge curves of Li/NALE 1/$LiCoO_2$ cell at different C-rates (b) rate capability of Li/NALE 1/$LiCoO_2$ cell (c) discharge curve of Li/NALE 1/$LiCoO_2$ cell at 0.2 C for 90 cycles (d) Columbic efficiency curve of Li/NALE 1/$LiCoO_2$ cell at 0.2 C rate

3.5 Electrochemical Impedance Spectroscopy

The electrochemical impedance, as well as kinetic behaviors of non-aqueous electrolytes, was analyzed using electrochemical impedance spectroscopy (EIS) in the frequency range of 100 mHz to 5 MHz with an alternating current signal amplitude of 10 mV at room temperature, and it was directly related to the charging and discharging process in LIB. Figure 4 (a) shows the Nyquist plot of the fresh cell (before cycling) using NALE 1 as an electrolyte at an open circuit voltage (OCV) of 2.9 V. Figure 4 (b) shows the Nyquist plot of the cell in the charged state (4.3 V) after 90 cycles. The fresh cell delivers a high impedance value of 223.62 ohm (Total cell resistance, R_{all}) with one semicircle at the higher frequency side and an inclined peak at lower frequency side. After the 90^{th} cycle, the impedance value of R_{all} was 171.35 ohm which consists of two semicircles at higher and middle-frequency range and peak at low-frequency side. Its corresponding equivalent circuit is given in figure 4 (c) and calculated parameters are mentioned in Table 3.

Here, R1 is the resistance of the electrolyte and cell components. The semicircle in the high-frequency range was attributed to the surface-film (sf) resistance and the charge-transfer (ct) resistance. However, only one semicircle was seen in the higher to middle frequency range indicating the effects due to sf and ct are not separable and mentioned as R2. The semicircle in the low-frequency range was attributed to the bulk (b) resistance and assigned as R3. A constant phase element (CPE) was used in the equivalent circuit instead of pure capacitance due to the observation of depressed semicircle, which indicates the inhomogeneous surface of the cathode material. The respective constant phase element of CPE1 represents the combined effect of surface-film and double-layer capacitance and CPE2 in the cycled cell represent the bulk capacitance. The CPE3 in the cycled cell was exhibited at very low frequencies and was associated with the Li-ion diffusion process in the cathode. The proposed equivalent circuit and the assignment of resistances and capacitances are consistent with the interpretation of impedance spectra on electrode materials [28].

The fitted data result shows that the value of R1 for fresh cell was 19.62 ohm which slightly decreased to 17.41 ohm after 90 cycles. In the meantime, in fresh cells, the impedance of R2 corresponding to the high-frequency semicircle was generally attributed to the passivating surface-film (Solid Electrolyte

Interface, SEI) that forms on the cathode. In cycled cells, the R2 reached 30.64 ohm which was smaller as compared to that of 204 Ohm for a fresh cell. This was due to the 'formation' of interface between electrolyte and electrode [14]. The bulk resistance of R3 was observed as 123.3 ohm. In cycled cell, the capacitance of CPE1 and CPE2 values were in 7.52 µF and 0.27 mF, respectively. The CPE1 value (in the order of mF) was much higher as compared to CPE2 (in the order of µF), because this includes not only the bulk impedance of the electrode material but also the electrolyte trapped in the electrode pores [44].
SHANGGUAN *et al.* [45], have studied a similar trend in impedance behavior on Li|$LiCoO_2$ cells with LiFSI and $LiPF_6$ after 6 cycles at 0.5 C rate at ambient temperature. The obtained results show the value of 1.5 Ohm (R_{el}), 113.5 Ohm (R_{sf}) and 105.8 Ohm (R_{ct}) for the LiFSI-based cell and 8 Ohm (R_{el}), 95.7 Ohm (R_{sf}) and 72.4 Ohm (Rct) for the $LiPF_6$-based cell. However, in the present investigation, interestingly the surface film resistance was very low even after 90 cycles, which points out its good capacity retention and lower polarization [45]. Based on our investigations, the new salt LiNfO based NALE 1 could be the potential candidate as electrolyte for LIBs and better alternative for commercial $LiPF_6$ based liquid electrolytes in the near future.

Table 3: Fitted resistance and capacitance values for the cell

SAMPLE	R1/Ω	R2/Ω	R3/Ω	R_{ALL}/Ω	CPE1/µF	CPE2/mF	CPE3/mF
Fresh cell (Before cycling)	19.62	204	-	223.62	8.76	-	16.55
After 90 cycle	17.41	30.64	123.3	171.35	7.52	0.27	10.16

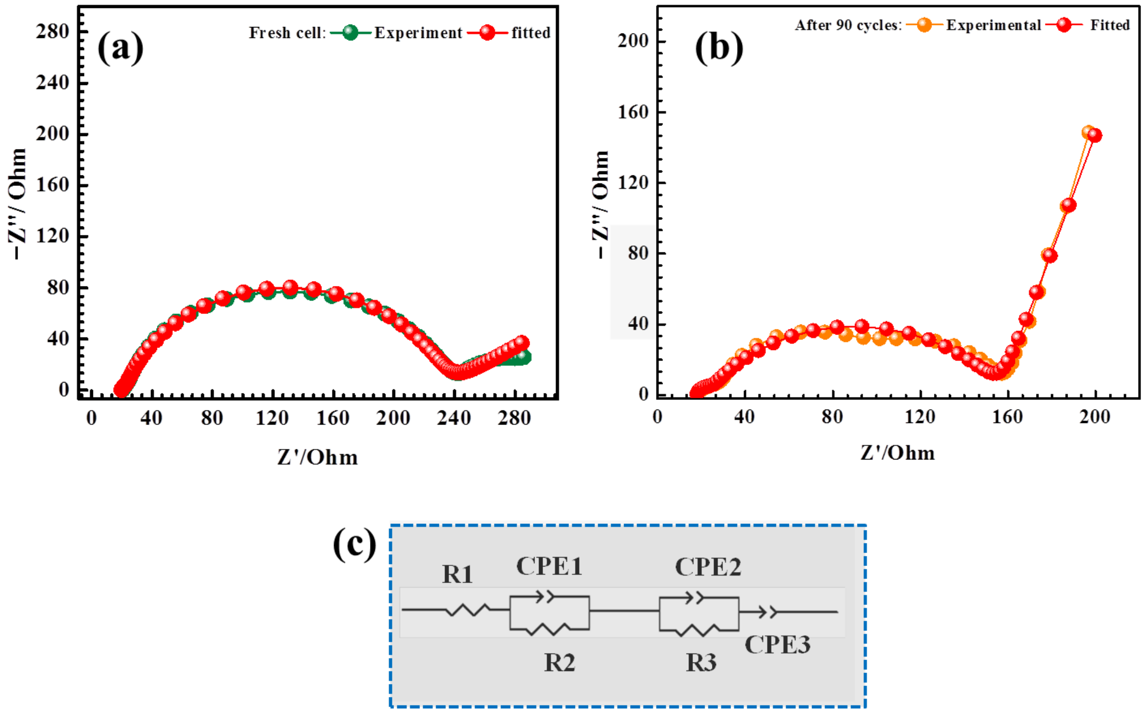

Figure 4: (a, b) Nyquist impedance plot of Li/NALE 1/$LiCoO_2$ cell before and after cycling (c) its corresponding equivalent circuit

4. CONCLUSIONS

The novel NALE electrolyte made from 0.1M LiNfO in the PC/DME binary solvent mixture shows the maximum ionic conductivity of 2.66 x 10^{-3} S cm^{-1} at ambient temperature for PC: DME ratio of 1:1. The above electrolyte shows the high electrochemical stability window of nearly 5 V making it as most suitable for high voltage applications. The Li/NALE 1/$LiCoO_2$ cell delivered a very high discharge capacity of 154 mA h g^{-1} at 0.1 C with better rate capability. This work opens up the possibility of widespread application of proposed LiNfO based non-aqueous liquid electrolytes in high voltage LIBs.

5. ACKNOWLEDGEMENTS

Hirankumar Gurusamy acknowledges BRNS, Department of Atomic Energy, Government of India for the financial support through the project (sanction number 2012/34/71/BRNS).

6. BIBLIOGRAPHY

[1] DING, J., WANG, H., LI, Z., *et al.*, “Peanut shell hybrid sodium ion capacitor with extreme energy–power rivals lithium ion capacitors”, *Energy and Environmental Sciences,*v. 8, pp. 941-955, March 2015.

[2] PRABU, M., SELVASEKARAPANDIAN, S., KULKARNI, A., *et al.,* “Structural, dielectric, and conductivity studies of yttrium-doped $LiNiPO_4$ cathode materials”, *Ionics,* v. 17, pp. 201-207, March 2011.

[3] AMBIKA, C., HIRANKUMAR, G., “Characterization of CH_3SO_3H-doped PMMA/PVP blend-based proton-conducting polymer electrolytes and its application in primary battery”, *Applied Physics A*, v. 122, pp. 113-123, February 2016.

[4] KRAUSE, L.J., LAMANNA,W., SUMMERFIELD, J., *et al.,”* Corrosion of aluminum at high voltages in non-aqueous electrolytes containing perfluoroalkylsulfonyl imides”; new lithium salts for lithium-ion cells, *Journal of Power Sources,* v. 68, pp. 320-325, March 1997.

[5] WILKEN, S., TRESKOW, M., SCHEERS, J., *et al.,* “Initial stages of thermal decomposition of $LiPF_6$-based lithium ion battery electrolytes by detailed Raman and NMR spectroscopy”, *RSC Advances,* v. 3, pp. 16359-16364, October 2013.

[6] ZHANG, H., FENG, W., NIE, J., *et al., ”*Recent progresses on electrolytes of fluorosulfonimide anions for improving the performances of rechargeable Li and Li-ion battery”, *Journal of Fluorine Chemistry,* v. 174, pp. 49-61, June 2015.

[7] KARUPPASAMY, K., REDDY, P.A., SRINIVAS, G., *et al.*, “An efficient way to achieve high ionic conductivity and electrochemical stability of safer nonaflate anion-based ionic liquid gel polymer electrolytes (ILGPEs) for rechargeable lithium ion batteries”, *Journal of Solid State Electrochemistry,* v. 955, pp. 1145-1155, April 2017.

[8] KARUPPASAMY, K., REDDY, P.A., SRINIVAS, G., *et al.*, “Electrochemical and cycling performances of novel nonafluorobutanesulfonate (nonaflate) ionic liquid based ternary gel polymer electrolyte membranes for rechargeable lithium ion batteries”, *Journal of Membrance Science,* v. 514, pp. 350-357, September 2016.

[9] ARAI, J., KATAYAMA, H., AKAHOSHI, H., *et al* “Binary Mixed Solvent Electrolytes Containing Trifluoropropylene Carbonate for Lithium Secondary Batteries”, *Journal of Electrochemical Society,* v. 149, pp. A217-A226, January 2002.

[10] GUO-RONG, H., JING-CHAO, C., ZHONG-DONG, P., *et al.,* “Enhanced high-voltage properties of $LiCoO_2$ coated with $Li[Li_{0.2}Mn_{0.6}Ni_{0.2}]O_2$”, *Electrochimica Acta*, v. 149 pp. 49-55, March 2014. 149 (2014) 49-55.

[11] LEE, C., KIM, J.H., BAE, J.Y., *et al “*Polymer gel electrolytes prepared by thermal curing of poly(vinylidene fluoride)-hexafluoropropene/poly(ethylene glycol)/propylene carbonate/lithium perchlorate blends”, *Polymer,* v. 44, pp. 7143-7155, November 2003.

[12] NANBU, N., TAKIMOTO, K., TAKEHARA, M., *et al.,”*Electrochemical properties of fluoropropylene carbonate and its application to lithium-ion batteries”, *Electrochemistry Communications*, v. 10, pp. 783-786, May 2008.

[13] XIANGBANG, K., RONG, Z., JING, W., *et al.*, “An Effective Electrolyte Strategy to Improve the High Voltage Performance of $LiCoO_2$ Cathode materials”, *ACS Applied Energy Materials,* v. 2, pp. 4683-4691, June 2019.

[14] TAN, K.S., REDDY, M.V., SUBBA RAO, G.V., *et al.,* “$AlPO_4$-coating on cathodic behaviour of $Li(Ni_{0.8}Co_{0.2})O_2$”, *Journal of Power Sources,* v. 141, pp. 129-142, February 2005.

[15] HONG-BO, H., SI-SI ZHOU, DAI-JUN ZHANG, *et al.,* “Lithium bis(fluorosulfonyl)imide (LiFSI) as conducting salt for nonaqueous liquid electrolytes for lithium-ion batteries: Physicochemical and electrochemical properties”, *Journal of Power Sources,* v. 196, pp. 3623-3632, April 2011.

[16] ZHAO, Y., WANG, J., YAN, Z., *et al.*, “Molar volumes and viscosities of $LiClO_4$ and LiBr in propylene carbonate + 1,2-dimethoxyethane mixed solvents at 298.15 K”, *Fluid Phase Equilibria,* v. 244, pp. 105-110, June 2006.

[17] ABOUIMRANE, A., DING, J., DAVIDSON, I., *et al* “Liquid electrolyte based on lithium bis-fluorosulfonyl imide salt: Aluminum corrosion studies and lithium ion battery investigations”, *Journal of Power Sources,* v. 189, pp. 693-696, April 2009.

[18] WALKER, C.W., COX J.D, SALOMON, M., *et al* “Conductivity and Electrochemical Stability of Electrolytes Containing Organic Solvent Mixtures with Lithium tris (Trifluoromethanesulfonyl) methide”, *Journal of Electrochemical Society,* v. 143, pp. L80-L82, January 1996.

[19] LAM, P.H., TRAN, A.T., WALCZYK, D.J., *et al.*, “Conductivity, viscosity, and thermodynamic properties of propylene carbonate solutions in ionic liquids”, *Journal of Molecular Liquids,* v. 246, pp. 215-220, November 2017.

[20] GHOSH, A., WANG, C., KOFINAS, P., *et al “*Block Copolymer Solid Battery Electrolyte with High Li-Ion Transference Number*”*, *Journal of Electrochemical Society,* v. 157, pp. A846-A849, May 2010.

[21] ZUGMANN, S., FLEISCHMANN, M., AMERELLER, M., *et al.*, “Measurement of transference numbers for lithium ion electrolytes via four different methods, a comparative study”, *Electrochimica Acta*, v. 56, pp. 3926-3933, April 2011.

[22] YAN, D., BAZANT, M.Z., BIESHEUVEL, P., *et al.*, “Theory of linear sweep voltammetry with diffuse charge: Unsupported electrolytes, thin films, and leaky membranes”, *Physical Review E,* v. 95, pp. 033303, March 2017.

[23] GIRARD, G.M.A., HILDER, M., ZHU, H., *et al.*, “Electrochemical and physicochemical properties of small phosphonium cation ionic liquid electrolytes with high lithium salt content”, *Physical Chemistry Chemical Physics*, v. 17, pp. 8706-8713, April 2015.

[24] ZARROUGUI, R., HACHICHA, R., RJAB, R., *et al.*, “1-Allyl-3-methylimidazolium-based ionic liquids employed as suitable electrolytes for high energy density supercapacitors based on graphene nanosheets electrodes”, *Journal of Molecular Liquids,* v. 249, pp. 795-804, January 2018.

[25] SCHRODER, K.W., DYLLA, A.G., BISHOP, L.D., *et al.*, “*Effects of Solute–Solvent Hydrogen Bonding on Nonaqueous Electrolyte Structure”*, *Journal of Physical Chemistry Letters,* v. 6, pp. 2888-2891, July 2015.

[26] TAKAMATSU, D., ORIKASA, Y., MORI, S., *et al.*, “Effect of an Electrolyte Additive of Vinylene Carbonate on the Electronic Structure at the Surface of a Lithium Cobalt Oxide Electrode under Battery Operating Conditions”, *Journal of Physical Chemistry C,* v. 119, pp. 9791-9797, April 2015.

[27] REDDY, M.V., SUBBA RAO, G.V., CHOWDARI, B.V.R., *et al* “Cathodic behaviour of NiO-coated $Li(Ni_{1/2}Mn_{1/2})O_2$”, *Electrochimica Acta*, v. 8, pp. 3375–3382, May 2005.

[28] REDDY, M.V., SUBBA RAO, G.V., CHOWDARI, B.V.R., *et al* “Preparation and Characterization of $LiNi_{0.5}Co_{0.5}O_2$ and $LiNi_{0.5}Co_{0.4}Al_{0.1}O_2$ by Molten Salt Synthesis for Li Ion Batteries”, *Journal of Physical Chemistry C,* v. 111, pp. 11712-11720, July 2007.

[29] SZU LUI TEY., REDDY M.V., SUBBA RAO G.V., *et al.*, “Synthesis, Structure, and Magnetic Properties of $[Li(H_2O)M(N_2H_3CO_2)_3]\cdot 0.5H_2O$ (M = Co,Ni) as Single Precursors to $LiMO_2$ Battery Materials”, *Chemistry of Materials,* v. 18, pp. 1587-1594, February 2006.

[30] ZHANG, L., MA, Y., CHENG, X., *et al.*, “Capacity fading mechanism during long-term cycling of over-discharged $LiCoO_2$/mesocarbonmicrobeads battery”, *Journal of Power Sources,* v. 293, pp. 1006-1015, October 2015.

[31] CAO, J., HU, G., PENG, Z., *et al.*, “Polypyrrole-coated $LiCoO_2$ nanocomposite with enhanced electrochemical properties at high voltage for lithium-ion batteries”, *Journal of Power Sources,* v. 281, pp. 49-55, May 2015.

[32] AURBACH, D., GAMOLSKY, K., MARKOVSKY, B., *et al.,”* On the use of vinylene carbonate (VC) as an additive to electrolyte solutions for Li-ion batteries”, *Electrochimica Acta,* v. 47, pp. 1423-1439, February 2002.

[33] YATABE, S., HORIBA, T., KUBOTA, K., *et al.*, “Effect of diphenylethane as an electrolyte additive to enhance high-temperature durability of $LiCoO_2$/graphite cells”, *Electrochimica Acta*, v. 270, pp. 120-128, April 2018.

[34] WANG, F., WU, Y., LU, K., *et al.*, “A sensitive voltammetric sensor for taxifolin based on graphenenanosheets with certain orientation modified glassy carbon electrode”, Sens. *Actuator B-Chem*. v. 208, pp. 188-194, March 2015.

[35] REDDY, M.V., PECQUENARD, B.,VINATIER, P., *et al.*, “Cyclic voltammetry and galvanostatic cycling characteristics of $LiNiVO_4$ thin films during lithium insertion and re/de-insertion”, *Electrochemistry Communications,* v. 955, pp. 409–415, March 2007.

[36] RAMADAN, H., BECHERIF, M.,CLAUDE F., *et al* “Extended kalman filter for accurate state of charge estimation of lithium-based batteries: a comparative analysis”, *Inernational Journal of Hydrogen Energy*, v. 42, pp. 29033-29046, November 2017.

[37] MAFTOON-AZAD, I., NAZARI F., “Anion-cation, anion-lithium, cation-lithium and ion pair-lithium interactions in alicyclic ammonium based ionic liquids as electrolytes of lithium metal batteries”, *Journal of Molecular Liquids,* v. 242, pp. 1228-1235, September 2017.

[38] DOKKO, K., NAKATA, N., KANAMURA, K., *et al* “High rate discharge capability of single particle electrode of $LiCoO_2$”, *Journal of Power Sources,* v. 189, pp. 783-785, April 2009.

[39] CHEN, Z., DAHN, J., “Methods to obtain excellent capacity retention in $LiCoO_2$ cycled to 4.5 V”, *Electrochimica Acta*, v. 49, pp. 1079-1090, March 2004.

[40] TANG, W., LIU, L., TIAN, S., *et al.*, “Nano-$LiCoO_2$ as cathode material of large capacity and high rate capability for aqueous rechargeable lithium batteries”, *Electrochemistry Communications*, v. 12, pp. 1524-1526, November 2010.

[41] MCLAREN,V.L., WEST, A.R., TABUCHI, M., *et al.*, “Study of the Capacity Fading Mechanism for Fe-Substituted $LiCoO_2$ Positive Electrode”, *Journal of Electrochemical Society*, v. 151, pp. A672-A681, May 2004.

[42] PARK, J.S., MANE, A.U., ELAM, J.W., *et al.*, “Amorphous Metal Fluoride Passivation Coatings Prepared by Atomic Layer Deposition on $LiCoO_2$ for Li-Ion Batteries”, *Chemistry of Materials,* v. 27, pp. 1917-1920, March 2015.

[43] ZUO, D., TIAN, G., CHEN, D., *et al.*, “Comparative study of Al_2O_3-coated $LiCoO_2$ electrode derived from different Al precursors: uniformity, microstructure and electrochemical properties”, *Electrochimica Acta*, v. 178, pp. 447-457, October 2015.

[44] REDDY, M.V., BRYAN LEE WEI WEN., KIAN PING, L., *et al.*, “Energy Storage Studies on $InVO_4$ as High Performance Anode Material for Li-Ion Batteries”, *`ACS Applied Materials & Interfaces,* v. 5, pp. 7777-7785, July 2013.

[45] XUEHUI, S., GUOFENG, J., FAQIANG, L., *et al.*, “Mixed salts of LiFSI and LiODFB for stable $LiCoO_2$-based batteries”, *Journal of Electrochemical Society,* v. 163, pp. A2797-A2802, October 2016.

ORCID

Hirankumar Gurusamy	https://orcid.org/0000-0002-1724-2001
Sakunthala Ayyasamy	https://orcid.org/0000-0002-9945-6272
Daries Bella	https://orcid.org/0000-0003-3207-5712